

Incipient Sensor Fault Impacts on Building Performance Through HVAC Controls – A Pilot Study

Yanfei Li¹, Yeobeom Yoon¹, Yeonjin Bae¹, Piljae Im¹, and Sangkeun Matt Lee¹

¹Oak Ridge National Laboratory, Oak Ridge, TN

Abstract

Sensors are crucial input components for HVAC controls. Studies show faults are common for buildings and HVAC systems. Sensors with faults will compromise the control performance regardless how advanced of the control algorithms. Majority studies assume the sensor fault to be constant the whole year. In reality, the sensor faults might evolve or develop with time, which is essentially the incipient (i.e. evolving) fault. The incipient sensor faults impacts remain a research gap. This study aims to investigate the incipient sensor fault impacts to control sequences of multi-zone VAV boxes and AHU system following the ASHRAE Guideline 36-2018: High-Performance Sequences of Operation.

Introduction

Building sector consumes more energy than the transportation and industrial sectors in United States. With requirements of reduced carbon emission worldwide, it is demanding to reduce the building energy consumption and carbon emissions. Controls in buildings have been proved for huge energy saving benefits (Y. Li et al. 2021; O'Neill et al. 2020; Wang and Ma 2008). Building control algorithms can be classified into three categories: supervisory control, local control, and rule-based control. Supervisory control aims to find the system level optimum performance for building operations. The local control has three algorithms in general: proportional (P), proportional-integral (PI), and proportional-integral-derivative (PID) controls. The rule-based control is more domain-specific and based on actual operation experience. However, control systems heavily rely on sensors to collect information on building and heating, ventilation, and air-conditioning (HVAC) systems to make control decisions. Faults are common in building operations (Y. Li and O'Neill 2019b). Sensors

could be operating under faulty conditions (e.g. sensor errors) due to various reasons. Sensors with errors will feed incorrect building status (e.g. indoor air temperature) to the control systems. This will lead the control system make unfavourable decisions which compromise the energy saving benefits (Bae et al. 2021; Y. Li and O'Neill 2018, 2019a; Lu et al. 2020).

For the sensor fault study, there are three major trends: fault detection and diagnostics (FDD), fault modelling and impacts, and fault prevalence. The sensor fault detection and diagnostics study started around 20 years ago (Du and Jin 2007). The most recent study is using the data-driven methods to detect sensor faults (T. Li et al. 2022). However, the FDD studies might generate false alarms for a fault not existing. There are emerging studies focusing on the fault model recent years, which include sensor faults modelling and impacts. There is a study investigated the fixed sensor error impacts on the demand control ventilation performance through stochastics approach. They assumed normal distribution for the sensor errors among 3,000 simulation cases, which each case has constant sensor error through the whole year. Their study showed the sensor errors have stronger impacts on demand control performance (Lu et al. 2020). Similarly, another study investigated the sensor impacts on building performance through stochastic sampling. Their study demonstrated the prioritized sensor impacts (Y. Li and O'Neill 2019a). Recently, the fault prevalence gains some attentions, which describes the percentage of components/systems with fault occurred at a given severity at a single point within a time period. This aspect remains a challenge, because the HVAC systems and components faults are depending on many factors, such as building types, HVAC systems, climate zones, operations, etc. This study reviewed the possible fault prevalence of HVAC systems (Kim et al. 2021). Another study investigated the fault prevalence in commercial buildings based on

multi-year building operation data (Ebrahimifakhar 2021).

It is remained a research gap for the appropriate sensor fault profile for different sensors. Based on the manufacturing recommendation, we classified the sensor errors into: fixed sensor error and incipient sensor error. The fixed sensor error is characterized by a constant deviation between desired and fault conditions. The incipient sensor error is the error evolving or changing with time. From practical perspectives, the sensor errors tend to be incipient errors. This study aims to investigate the incipient sensor error impacts on HVAC controls (ASHRAE-36 controls) through simulation model, as a pilot study. The ASHRAE-36 control is practical control algorithm proven by studies and practical implementations (ASHRAE 2022; Hydeman, Taylor, and Eubanks 2015; Pradhan et al. 2021). The analysis will be focusing on the building energy consumption and thermal comfort. The stochastic samplings of sensor errors are injected to the model. The large-scale simulations were implemented in the cloud.

Methods

Simulation model

To evaluate the impact of the sensor impacts on control performance, a simulation study was established. The building model is based on Flexible Research Platform (FRP-2) at Oak Ridge National Laboratory. The building is a two-storey multi-zone office building. The rooftop unit system provides cooling and heating to the building. The main heating coil is a gas heating coil. Each zone is served by a variable air volume box with an electricity reheat coil. The rooftop unit (RTU) and variable air volume (VAV) box controls adopted the practical control sequences from ASHRAE Guideline 36-2018: High-Performance Sequences of Operation. For sensors, the incipient (time-changing) sensor errors, including bias sensor error and precision sensor error, are the inputs of interest. The simulation flowchart is shown in Figure 1.

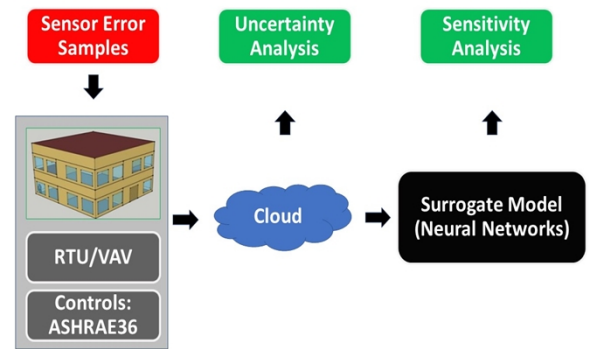


Figure 1 Simulation flowchart

Cloud simulation

In order to investigate the sensor impacts, the cloud simulations were conducted in Azure Platform. A total of 3,600 simulation cases were performed on the cloud. Each case was injected time-changing sensor errors (bias and precision) as inputs. The outputs are energy consumption and thermal comfort (e.g., the predicted percentage of dissatisfied occupants [PPD]). Based on the simulation results, uncertainty analysis and sensitivity analysis were performed. Figure 2 shows the cloud simulation workflow and detailed information of each step of the cloud workflow is as follows:

1. A Python script (Figure 3) was developed to generate 3,600 simulation input data files (IDF files). Each IDF file was associated with a Python class of sensor errors through Python EMS. During the simulation, at each time step, a new sensor error (including bias and precision) was injected into the ideal sensor readings from EnergyPlus.
2. After 3,600 cases were generated, they were uploaded to the Azure cloud platform.
3. In the Azure cloud platform, a bash script selected the appropriate virtual machine configurations (e.g., memory and hard drive) and a number of virtual machines.
4. The Azure cloud provided a job scheduler, which automatically distributed all 3,600 cases across 300 nodes.
5. The simulation ran automatically until all cases were accomplished.
6. Finally, all the results were selected to set up the data sets (inputs and outputs) to create the black-box models.

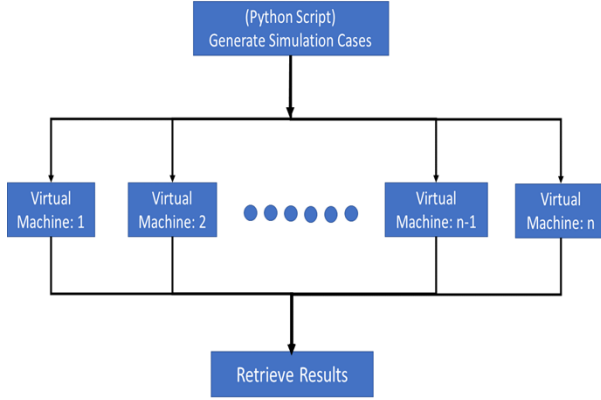


Figure 2 Cloud simulation workflow

```
for time in range(0, 365*24*60):
    sensor_readings = get_building_states(energyplus_api)
    sensor_err_bias = generate_sensor_err_bias()
    sensor_err_precision = generate_sensor_err_precision()
    sensor_err_tot = sensor_err_bias + sensor_err_precision
    overwrite_sensor_readings(energyplus_api)
    calc_hvac_energy_consumption(energyplus_api)
```

Figure 3 Pseudo Code for Sensor Error Injection

Sensor sets

Based on the ASHRAE-36 control logics for VAV box and AHU, five sensor types were selected for the following reasons: (1) the indoor air (IA) temperature is the most important variable to be controlled to meet the heating and cooling set-points temperature; (2) the IA temperature is directly impacted by the VAV box supply air (SA) temperature and SA flow rate from the control perspective; (3) RTU system-level operation also directly impacts the VAV box operations; (4) RTU outdoor air (OA) temperature and SA temperature are significant in determining the system-level energy consumption. The sensor types are listed in Table 1.

Table 1 Selected sensor list

Location	Measurement	Priority	Note
Room	IA temperature	1	Indoor air temperature
VAV box	SA temperature	1	VAV box supply air temperature
VAV box	SA flow rate	1	VAV box supply air flow rate
RTU	OA temperature	1	Outdoor air temperature
RTU	SA temperature	1	Supply air temperature

Sensor errors

The total sensor error comprises two components (Bae et.al 2021): bias error and precision error. For a sensor,

there is an ideal reading (or true reading) at a time step, as shown in the black line of Figure 4. The bias error is the system deviation from the ideal readings, as shown in the green dotted line of Figure 4. The precision error is the random deviation from the average sensor readings, on top of bias or true readings, as shown in the blue lines of Figure 4.

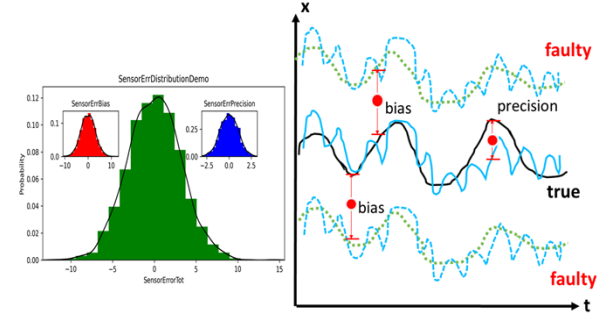


Figure 4. Sensor error diagram

The bias error evolves bigger or smaller with time as external environment changes. The fault profiles of sensor bias differ with the type of sensors (e.g temperature sensor, flow sensor, and pressure sensor). The bias might develop slowly, or progress rapidly. The mathematical expression of such fault profile is given as:

$$X_f(t) = X_o(t) + X_{bias}(t) + X_{precision}(t)$$

Where,

X_f is the fault reading,

X_o is the ideal reading,

X_{bias} is the bias error, and

$X_{precision}$ is the precision error.

The bias error is normal distribution with certain standard deviation. The expression is given as:

$$X_{bias}(t) = N(0, \sigma_{bias})$$

Similarly, the precision error is also normal distribution, with certain standard deviation. The expression is given as:

$$X_{precision}(t) = N(0, \sigma_{precision})$$

The standard deviations for the bias and precision of different sensors are based on two aspects: (1) sensor manufacturing recommended error(Texas Instruments 2022). (2) engineering judgement. The final picked threshold for standard deviations are shown in Table 2.

Table 2 Threshold for Standard Deviations

Location	Measurement	Std Bias	Std Precision
Room	IA temperature (°C)	1	0.1

VAV box	SA temperature (°C)	1	0.1
VAV box	SA flow rate (m ³ /s)	0.005	0.0005
RTU	OA temperature (°C)	1	0.1
RTU	SA temperature (°C)	1	0.1

Uncertainty analysis

To understand how are impacts of sensor errors on aggregated energy consumption, the uncertainty analysis were performed. The flowchart is shown in Figure 5.

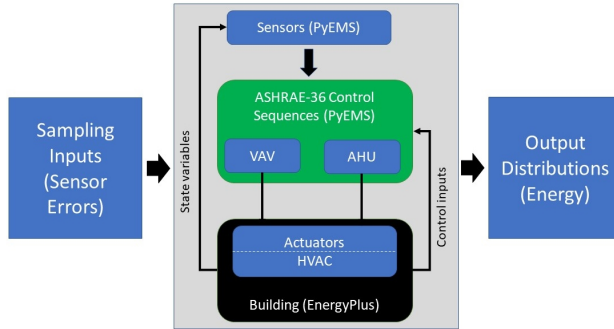


Figure 5 Uncertainty analysis flowchart

The distributions of the site energy consumption and OAT sensor error standard deviation are shown in Figure 6. The site energy consumption is 334000 ~ 346,000 kBtu/year (97.9 kWh/year ~101.4 kWh/year) based on the distribution of sensor total errors. The variation of total site energy consumption was 12000 kBtu/year (3.52 kWh/year), which is 3.5% of the average site energy consumption (340083 kBtu/year; 99.7 kWh/year).

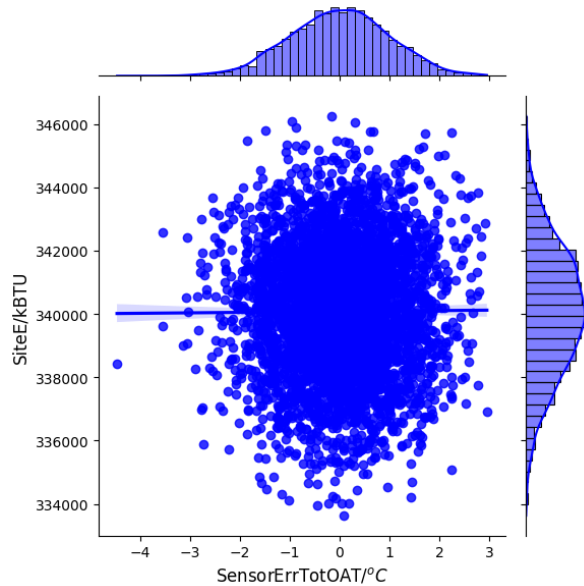


Figure 6 AHU-OAT sensor error and site energy

Similarly, the distributions of the cooling energy consumption and air handling unit outdoor air temperature (AHU-OAT) sensor error distributions are shown in Figure 7. Other aggregated energy consumptions (heating energy, cooling energy, and fan energy) show a pattern similar to that of site energy. Due to the page limitations of the conference paper, other energy items are not shown here. Overall, the energy consumption distribution has a Gaussian shape. The distribution shows that the outputs and sensor errors have a totally nonlinear relationship.

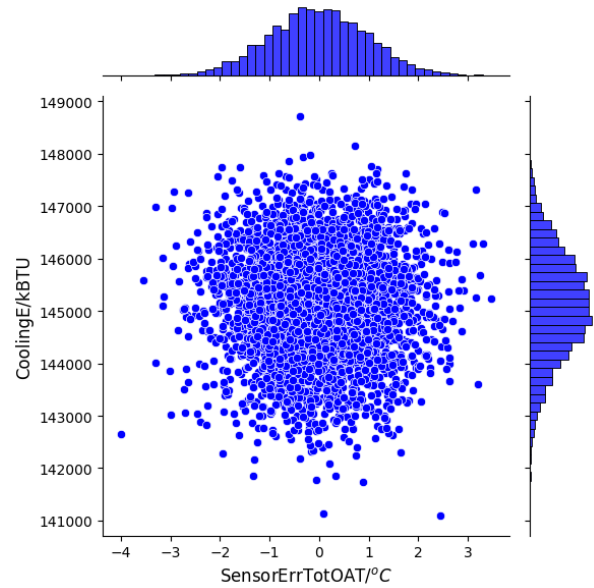


Figure 7 AHU-OAT sensor error and cooling energy

Sensitivity analysis

The sensitivity analysis was performed to rank the most critical sensors in this study. The sensitivity is based on global black-box method (Long Short Term Memory Recurrent Neural Network). The flowchart is shown in Figure 8.

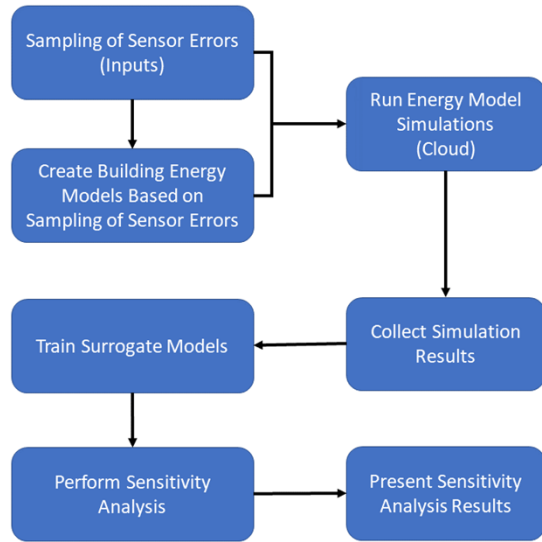


Figure 8 Sensitivity analysis flowchart

Based on the simulation results, both AHU-level and zone-level sensitivity analyses were performed. The results are presented in the following subsections. For zone-level analysis, there are two floors, and each floor has five zones. They have similar patterns regarding the sensitivity analysis. One zone from each floor (zone 102 and zone 204) was selected to demonstrate the sensitivity analysis.

System-level sensitivity analysis

The actual cooling capacity and power consumption were studied at the AHU-level. Figure 9 illustrates the sensitivity index for cooling capacity. The cooling capacity is most sensitive to the random errors of the SA and OA temperature sensors. These errors have the most significant impacts on cooling capacity, followed by the total errors of SA and OA temperature sensors, and then the bias errors of SA and OA temperature sensors.

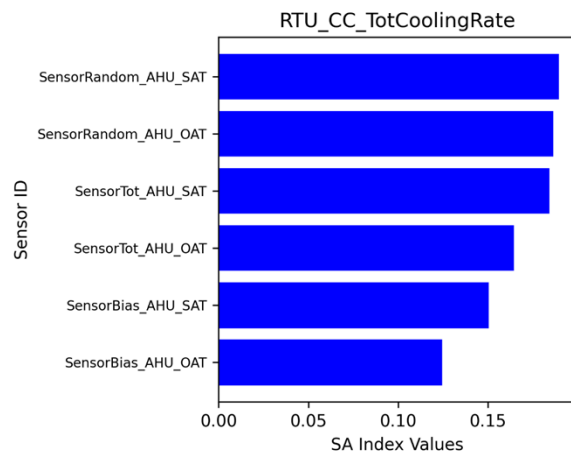


Figure 9 Sensitivity analysis for RTU cooling rate

Figure 10 illustrates the sensitivity index for RTU power demands. The sensor impacts are similar to the actual cooling capacity. The random errors for the SA and OA temperature sensors are the most significant, followed by total errors, and then bias errors. Because there is a linear relationship between the actual cooling rate and power demands for RTU, the sensitivity index shows the consistent impacts from those sensors.

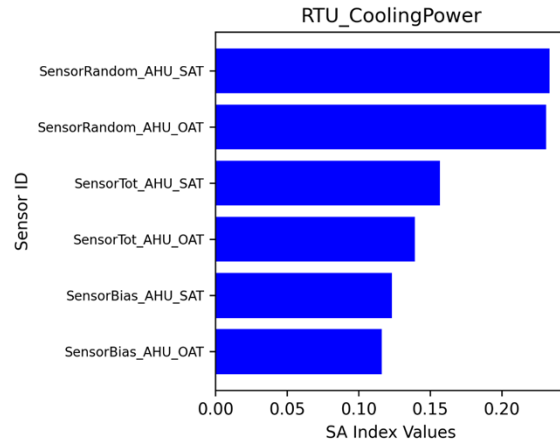


Figure 10 Sensitivity analysis for RTU cooling power

Zone 204 sensitivity analysis

At the zone-level, four energy consumption items (indoor air temperature, zone sensible heating energy, zone sensible cooling energy, and reheat coil energy) and one thermal comfort item (PPD) were selected. Figure 11 shows the ranking of sensitivity index for indoor air temperature. Overall, the system- and zone-level sensors impacted the indoor air temperature. The sensor with the highest sensitivity index was the indoor air temperature sensor with random error. The random errors are the most influential, followed by total errors, and then bias errors. Figure 12 shows the ranking of sensitivity index for zone sensible heating energy. The indoor air temperature sensor with random error has the highest sensitivity index. Figure 13 shows the zone sensible cooling energy impacts from the sensors. Figure 14 shows the impacts to reheat coil energy. Figure 15 shows the sensitive index ranking for PPD. Across zone 204 output items, the random errors consistently have stronger impacts.

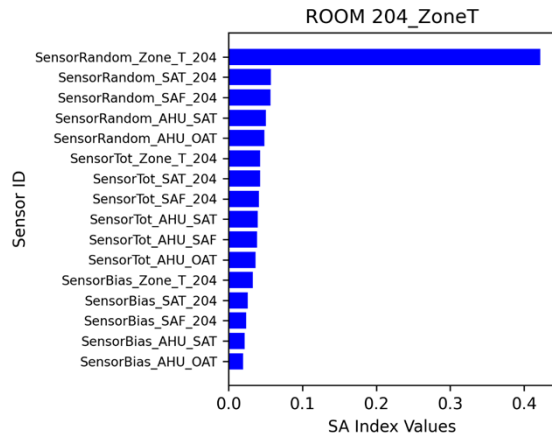


Figure 11 Sensitivity analysis for indoor air temperature of the zone 204

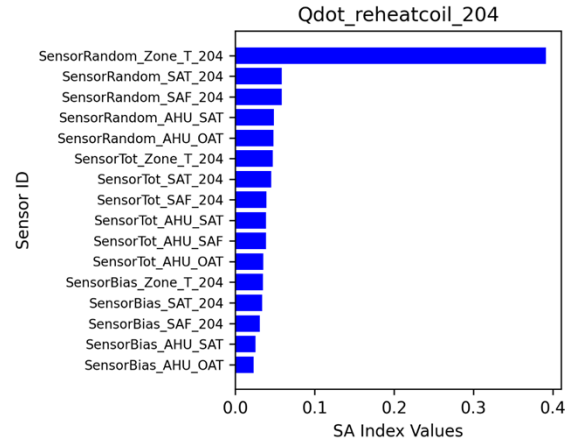


Figure 14 Sensitivity analysis for reheat coil energy of the zone 204

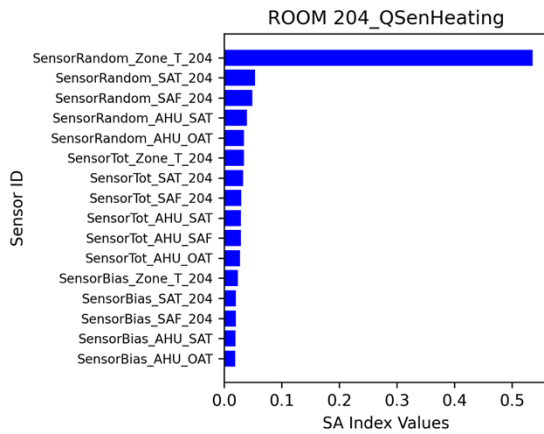


Figure 12 Sensitivity analysis for sensible heating energy of the zone 204

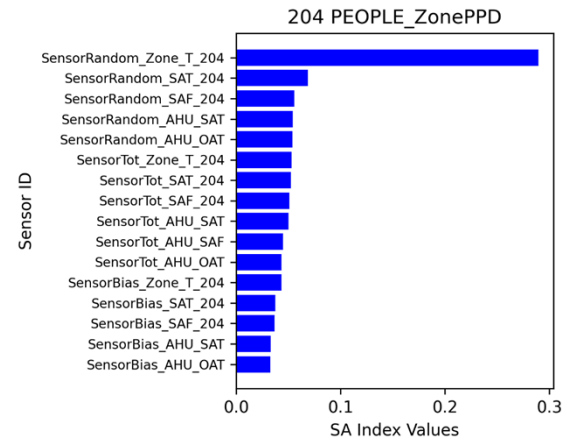


Figure 15 Sensitivity analysis for PPD of the zone 204

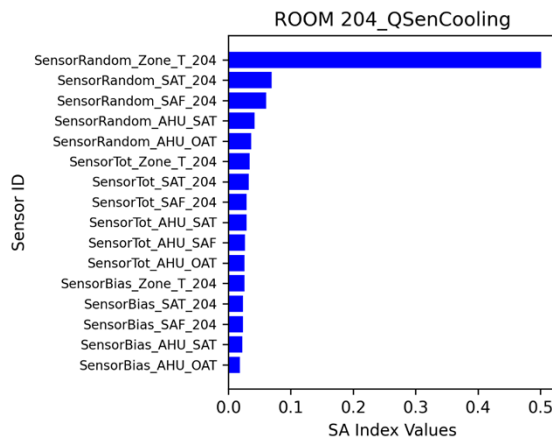


Figure 13 Sensitivity analysis for sensible cooling energy of the zone 204

Zone 102 sensitivity analysis

Sensitivity analysis for zone 102 was performed similarly to that of zone 204. The impacts of sensor errors on four energy consumption variables (indoor air temperature, zone sensible heating energy, zone sensible cooling energy, and reheat coil energy) and one thermal comfort item (PPD) were demonstrated. Figure 16 shows the ranking of sensitivity index for indoor air temperature. The system-level sensors and zone-level sensors impacted the indoor air temperature. The indoor air temperature sensor with random error had the highest sensitivity index. Figure 17 shows the ranking of sensitivity index for zone sensible heating energy. The indoor air temperature sensor with random error had the highest sensitivity index. Figure 18 shows the zone sensible cooling energy impacts from the sensors. Figure 19 shows the impacts to reheat coil energy. Figure 20 shows the sensitivity index ranking for PPD. Across

zone 102 output variables, random errors consistently have stronger impacts.

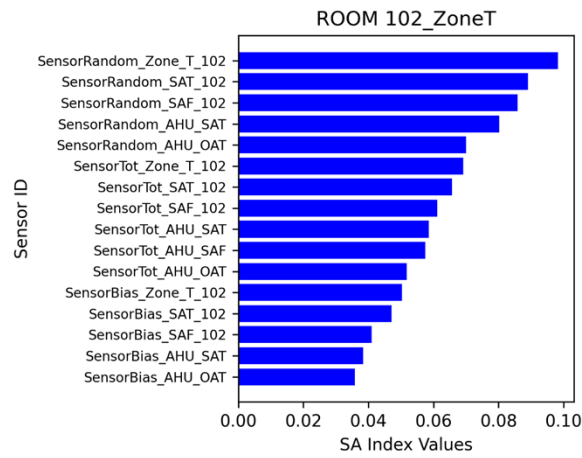


Figure 16 Sensitivity analysis for indoor air temperature of the zone 102

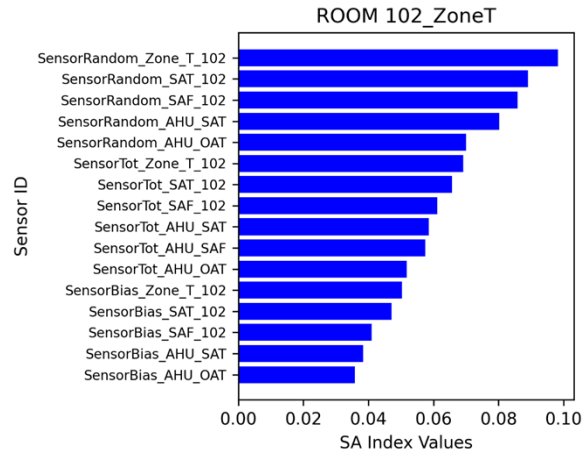


Figure 17 Sensitivity analysis for sensible heating energy of the zone 102

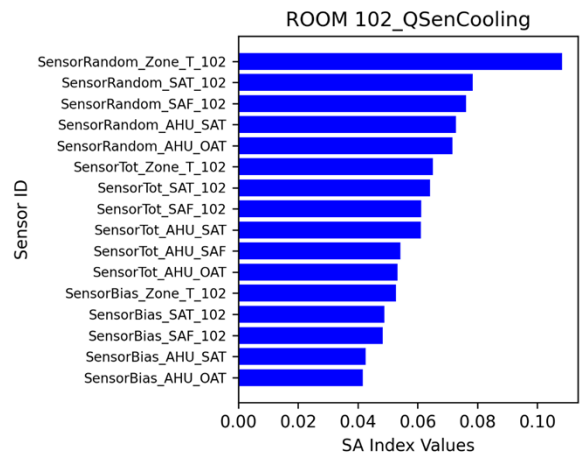


Figure 18 Sensitivity analysis for sensible cooling energy of the zone 102

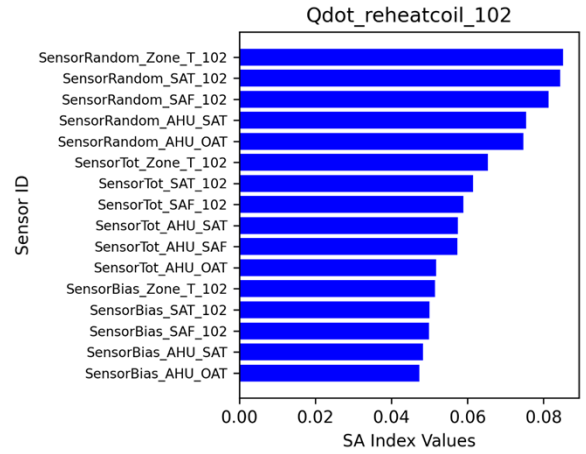


Figure 19 Sensitivity analysis for reheat coil energy of the zone 102

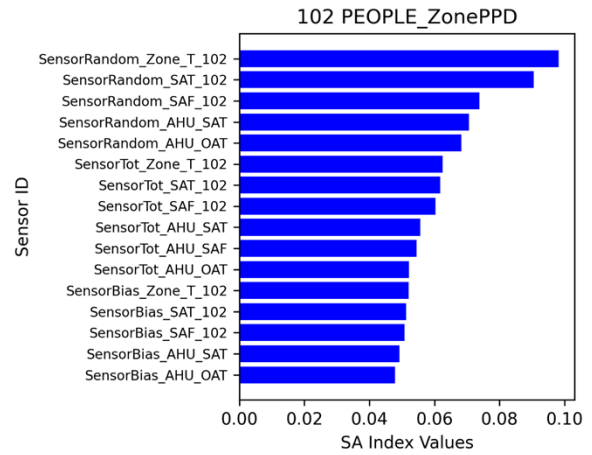


Figure 20 Sensitivity analysis for PPD of the zone 102

Conclusion

This study investigated the preliminary sensitivity analysis for energy consumption and thermal comfort with respect to sensor errors. The sensor errors had two components: bias error and precision (random) error. The sensor samplings were performed with normal distributions.

The energy consumption was classified into system levels (cooling capacity and power demands) and zone levels (indoor air temperature, zone sensible heating energy, zone sensible cooling energy, and zone reheat coil energy). The thermal comfort (PPD) at the zone level was also investigated.

The cloud simulations were conducted based on the sensor samplings and 3,600 simulation cases. The results were collected to train surrogate models for sensitivity analysis.

The uncertainty and sensitivity analyses were conducted with respect to sensor errors and energy/thermal comfort variables. The uncertainty analysis showed that the

sensor errors and energy consumptions have a nonlinear relationship. The energy consumptions have wide distributions compared with the baseline model with sensor error uncertainties.

The sensitivity analysis was performed for both system and zone levels. At the system level, the random errors for SA and OA temperature sensors have the most significant impacts. At the zone level, the random errors are the most influential, followed by total errors, and then bias errors.

Both the uncertainty analysis and sensitivity analysis show that sensor error/fault can not be simply ignored. It is extremely important to calibrate the sensors.

In the future, two major items will be explored: (1) other sensitivity analysis methods will be explored for comparative analysis, and other surrogate models might be explored. (2) fault analysis will be conducted considering sensor errors. Due to the limitations of conference paper, more results will be demonstrated in the journal paper.

Acknowledgment

This material is based upon work supported by the US Department of Energy's (DOE's) Office of Science and Building Technologies Office (BTO). This research used resources of Oak Ridge National Laboratory's Building Technologies Research and Integration, which is a DOE Office of Science User Facility. This manuscript has been authored by UT-Battelle LLC under contract DEAC05-00OR22725 with DOE. The US government retains and the publisher, by accepting the article for publication, acknowledges that the US government retains a nonexclusive, paid-up, irrevocable, worldwide license to publish or reproduce the published form of this manuscript, or allow others to do so, for US government purposes.

Nomenclatures

Nomenclature	Definition
X_f	Fault reading
X_o	Ideal reading
X_{bias}	Bias error
$X_{precision}$	Precision error
σ_{bias}	Standard deviation of bias error
$\sigma_{precision}$	Standard deviation of precision error

References

ASHRAE. 2022. "ASHRAE Guideline 36-2018: High-Performance Sequences of Operation."

Bae, Yeonjin et al. 2021. "Sensor Impacts on Building and HVAC Controls: A Critical Review for Building Energy Performance." *Advances in Applied Energy* 4: 100068.

Du, Zhimin, and Xinqiao Jin. 2007. "Detection and Diagnosis for Sensor Fault in HVAC Systems." *Energy Conversion and Management* 48(3): 693–702.

Ebrahimifakhar, Amir. 2021. "Investigation of the Prevalence of Faults in the Heating, Ventilation, and Air-Conditioning Systems of Commercial Buildings." The University of Nebraska-Lincoln.

Hydeman, Mark, Steven T. Taylor, and Brent Eubanks. 2015. "Control Sequences & Controller Programming." *ASHRAE Journal* 57(3): 58–62.

Kim, Janghyun et al. 2021. "Research Challenges and Directions in HVAC Fault Prevalence." *Science and Technology for the Built Environment* 27(5): 624–40.

Li, Tingting et al. 2022. "A Hierarchical Object Oriented Bayesian Network-Based Fault Diagnosis Method for Building Energy Systems." *Applied Energy* 306: 118088.

Li, Yanfei et al. 2021. "Grey-Box Modeling and Application for Building Energy Simulations-A Critical Review." *Renewable and Sustainable Energy Reviews* 146: 111174.

Li, Yanfei, and Zheng O'Neill. 2018. "A Critical Review of Fault Modeling of HVAC Systems in Buildings." In *Building Simulation*, Springer, 953–75.

Li, Yanfei, and Zheng O'Neill. 2019a. "An Innovative Fault Impact Analysis Framework for Enhancing Building Operations." *Energy and Buildings* 199: 311–31.

Li, Yanfei, and Zheng O'Neill. 2019b. "Simulation Based Fault Impact Analysis for the Secondary School in the US." *ASHRAE Transactions* 125(2).

Lu, Xing, Zheng O'Neill, Yanfei Li, and Fuxin Niu. 2020. "A Novel Simulation-Based Framework for Sensor Error Impact Analysis in Smart Building Systems: A Case Study for a Demand-Controlled Ventilation System." *Applied Energy* 263: 114638.

- O'Neill, Zheng D. et al. 2020. "Energy Savings and Ventilation Performance from CO₂-Based Demand Controlled Ventilation: Simulation Results from ASHRAE RP-1747 (ASHRAE RP-1747)." *Science and Technology for the Built Environment* 26(2): 257–81.
- Pradhan, Ojas et al. 2021. "Dynamic Bayesian Network-Based Fault Diagnosis for ASHRAE Guideline 36: High Performance Sequence of Operation for HVAC Systems." In *Proceedings of the 8th ACM International Conference on Systems for Energy-Efficient Buildings, Cities, and Transportation*, , 365–68.
- Texas Instruments. 2022. "Improving Accuracy in Temperature & Humidity Measurements." https://www.ti.com/lit/ml/slyp718/slyp718.pdf?ts=1648823132403&ref_url=https%253A%252F%252Fwww.google.com%252F.
- Wang, Shengwei, and Zhenjun Ma. 2008. "Supervisory and Optimal Control of Building HVAC Systems: A Review." *HVAC&R Research* 14(1): 3–32.